

INVESTIGATING LUNAR TOPOGRAPHIC PROPERTIES AT DIFFERENT SPATIAL SCALES USING DATA FROM THE LUNAR ORBITER LASER ALTIMETER AND THE WAVELET LEADERS METHOD.

M. Lemelin^{1,2}, M. Daly¹, and A. Delière³, ¹Center for Research in Earth and Space Science, York University, 4700 Keele St, Toronto, On, Canada M3J 1P3, lemelin@yorku.ca, ²Département de Géomatique appliquée, Université de Sherbrooke, Canada, ³Department of Electrical Engineering & Computer Science, University of Liège, Belgium.

Introduction: Various approaches exist to study the roughness of planetary bodies. The most commonly used focus on characterizing the roughness spatially by deriving statistics such as the root mean squared (RMS), median absolute or median differential slope, the RMS height, or the Hurst exponent [e.g., 1-5]. Other approaches focus on characterizing the roughness in frequency space, such as those using Fourier transforms.

Wavelet-based analyses have the advantage of characterizing the surface roughness both spatially and in frequency, but have been rarely used in a planetary science context so far. The Mexican Hat Wavelet Transform (MHWT) has been used to characterize the roughness of Mars in 1D using topographic profiles [6], while the Wavelet Leaders Method (WLM) has been used to characterize the roughness of Mars in 1D and in 2D using gridded topographic data [7]. Results from the 1D roughness characterization of Mars using the WLM are in agreement with the results using the MHWT and statistical approaches [e.g., 1-2], while the 2D roughness characterization of Mars was the first of its kind.

In this study, we use and refine the WLM used by [7] to study the roughness of the Moon both spatially and in frequency in 1D using gridded topographic data from the Lunar Orbiter Laser Altimeter (LOLA). The 1D WLM is an iterative process that calculates wavelet components at various spatial scales for a given vector of data, and investigates the wavelet leaders at each scale. These wavelet leaders are then used to determine (1) what are the different scaling regimes present in each longitudinal or latitudinal data profile (*i.e.*, at which scales or spatial resolution changes in what governs topographic processes occur), (2) whether the data at a given latitude or longitude is monofractal or multifractal, and (3) what is the value of its Hölder exponent.

Dataset : We used topographic data from LOLA that has been gridded and projected into a simple cylindrical projection (PDS3, V1.05) at 1024 ppd (or ~30 m/pixel), which is the highest spatial resolution currently available for the whole Moon. We downloaded individual tiles of 15° in latitude by 30° in longitude to obtain data for the whole globe. We then analyzed each of the 184,320 lines (latitudinal roughness) and 368,640 columns (longitudinal roughness) of data. The WLM uses data of size 2^x as input, so we downsampled each line of data (368,640 pixels) to 2^{18} (262,144) pixels, and each column of data (184,320 pixels) to 2^{17} (131,072) pixels. This corresponds to a spatial resolution of 728 ppd or ~41 m/pixel.

Methods: The wavelet components at various spatial scales for a given vector of data are first calculated as follows. The topographic signal of pixel i and its neighbors at scale j (2^x pixels) is compared to a theoretical wavelet (here a 3rd order Daubechies), yielding two components that each have 2^{x-1} pixels: the wavelet coefficients and the scaling coefficients. The former contain the high-frequency information (analogous to detrended topographic data) which is temporarily set aside for subsequent analysis. The latter contain the low-frequency information (analogous to the topographic data itself) which is used as input for the subsequent comparison between the “topographic” data and the theoretical wavelet at scale $j+1$. This process is done iteratively until there are 2^0 pixels left.

The wavelet “leaders” at each spatial scale are then identified. To do so, the wavelet coefficients obtained at each scale are compared using a dyadic cube; the maximum absolute value of the wavelet coefficient for pixel $i-1$ to $i+1$ at scale j and all finer scales is the wavelet leader value retained for pixel i at scale j .

The wavelet leaders are used to identify the different scaling regimes in a given vector of data via the structure function S :

$$S(j, q) = 2^{-j} \sum_{\lambda} d_{\lambda}^q$$

where j is the scale, λ is the dyadic cube, d_{λ} is the wavelet leader for that dyadic cube, and q is the order of the structure function. In practice, this can be done by (1) plotting $\log_2 S(j, q)$ versus j (Fig. 1), and (2) identifying the absolute value of the curvature on that plot, where the highest curvature value(s) represent the likeliest scale break(s).

The scaling function n is used to determine if the scaling regimes have a mono- or a multifractal behavior:

$$n(q) = \lim_{j \rightarrow +\infty} \frac{\log S(j, q)}{\log 2^{-j}}$$

In practice, this can be done by (1) plotting $n(q)$ versus q for various values of q (here from -2 to 2) for each scaling regime, and (2) calculating the correlation r between the n and its regression. The data has a monofractal nature if r is close to 1. Here we considered the data monofractal if $r > 0.98$, and multifractal if $r \leq 0.98$ as in [7]. If the data is monofractal, the slope of $n(q)$ versus q coincides with the Hölder exponent and characterizes its irregularity. If the data is multifractal, the slope gives the dominant Hölder exponent but does not fully represent the fractal properties of the signal.

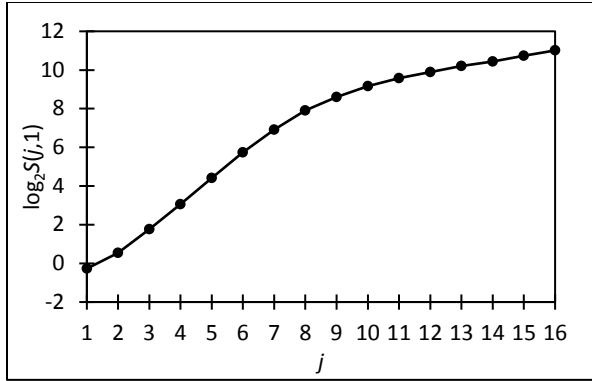


Figure 1. Plot of $\log_2 S(j,q)$ versus j (where $q=1$) for a given line of topographic data (at 50°N) used to identify the different scaling regimes occurring at that latitude.

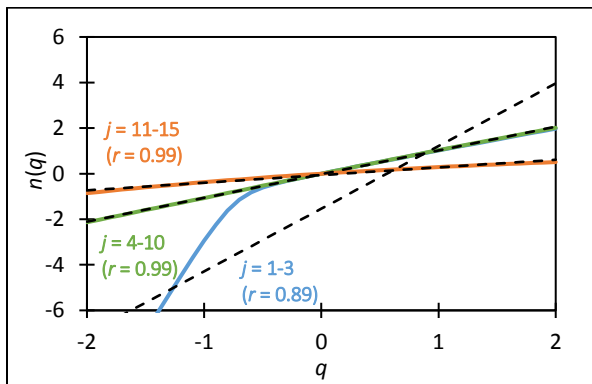


Figure 2. Plot of $n(q)$ versus q for the three scaling regimes (solid lines) identified at 50°N and their corresponding best linear fit (dashed lines).

Results and conclusion: Our preliminary results consist in the 1D roughness analysis for each latitudinal profile. S was calculated for a sample of profiles (every degree) to determine what are the different scaling regimes. We found that while the values vary slightly, scale breaks occur most often at $j = 3, 10,$ and $15,$ corresponding to spatial resolutions of 659 m/pixel, 84 and

$2,700$ km/pixel. They indicate that three scaling regimes are generally present in latitude at the discrete scales investigated here: $j = 1-3$ ($165-659$ m/pixel), $j = 4-10$ ($1-84$ km/pixel), and $j = 11-15$ ($169-2,700$ km/pixel). The scale breaks identified at $j = 3$ and 15 are still under investigation as data from fewer scales were involved in the computation of the curvature. The smallest scaling regime is consistent with [5] who found that within the baselines they investigated (~ 17 m to ~ 2.7 km), competing surface processes mostly occurs near 1 km. The two larger scaling regimes have not been studied previously. We hypothesize that the intermediate scaling regime ($1-84$ km/pixel) is characterized by the formation of simple and complex craters, whereas the largest scaling regime ($169-2,700$ km/pixel) is characterized by the formation of impact basins up to the largest on the Moon, the South Pole-Aitken basin ($D \sim 2,500$ km). At all latitudes the smallest scaling regime has a multifractal behavior, while the intermediate scaling regime has a monofractal behavior. The largest scaling regime has a multifractal behavior in the maria ($\sim 25^\circ\text{S}-65^\circ\text{N}$, mean Hölder = 0.34), and a monofractal behavior in the South Pole-Aitken basin (mean Hölder = 0.25) (Fig. 3).

The characterization of the 1D roughness for longitudinal profiles is underway. The characterization of the 2D roughness will be undertaken next, which will allow to determine the scale breaks, the fractal behavior, and the Hölder exponent value for each pixel rather than for vectors of data. This will allow a more precise characterization of the surface roughness, especially by investigating the differences between highlands and maria.

References: [1] Kreslavsky M. and Head J. (2000) *JGR*, *105*, 26695-26711. [2] Orosei R. et al. (2003) *JGR*, *108*, 8023. [3] Aharonson O. and Schorghofer N. (2006) *JGR*, *111*, E11007. [4] Yokota Y. et al. (2008) *LPSC 39*, abstract #1921. [5] Rosenburg M. A. et al. (2011) *JGR*, *116*, E02001. [6] Malamud B. and Turcotte D. (2001) *JGR*, *108*, 17497-17504. [7] Deliége A. et al. (2017), *PSS*, *136*, 46-58.

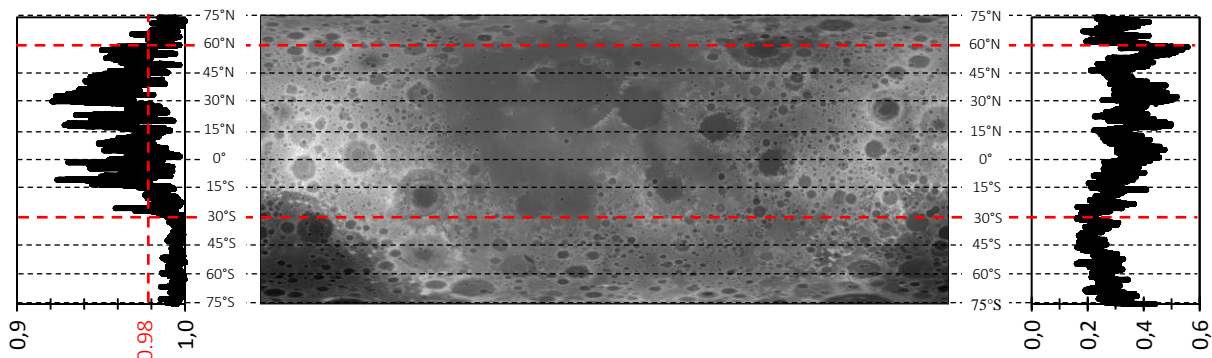


Figure 3. Results from the 1D roughness analysis for each latitudinal profile (line of data) for the largest scaling regime $j = 11-15$ ($169-2,700$ km/pixel). Left: correlation coefficients between $n(q)$ versus q and the best linear fit. Middle: LOLA topographic data shown between 75°S and 75°N . Right: the corresponding Hölder exponents.